

Pulsar timing and its applications

R. N. Manchester

CSIRO Astronomy and Space Science, PO Box 76, Epping NSW 1710, Australia

E-mail: dick.manchester@csiro.au

Abstract. Pulsars are remarkably precise “celestial clocks” that can be used to explore many different aspects of physics and astrophysics. In this article I give a brief summary of pulsar properties and describe some of the applications of pulsar timing, including tests of theories of gravitation, efforts to detect low-frequency gravitational waves using pulsar timing arrays and establishment of a “pulsar timescale”.

1. Introduction

Pulsars are remarkably precise “celestial clocks”. They are believed to be rotating neutron stars that send out beams of radio, optical, X-ray and γ -ray emission which we observe as pulses when they sweep across the Earth. About 2600 pulsars are currently known, almost all of which lie within our Galaxy.¹ The observed pulse periods range between 1 ms and 15 s, with most lying between 0.3 s and 3 s, the so-called “normal pulsars”. The “millisecond pulsars” (MSPs) form a distinct group, most with periods in the range 1 ms to 10 ms. Although pulsar periods (P) are very stable and predictable, they are not constant. Most pulsars are powered by their rotational kinetic energy and, as they lose energy to relativistic particle winds and radiation, they slow down. The rate of slowdown, \dot{P} , and other pulsar parameters can be determined using pulse time-of-arrival (ToA) measurements made over long intervals. MSPs are also distinguished by their very small \dot{P} s, around five orders of magnitude smaller than \dot{P} s for normal pulsars, and by the fact that most are in a binary orbit with another star. These different properties result from the very different evolutionary path followed by MSPs in which a central feature is spin-up of an old neutron star by accretion from a companion star [2].

In this review, we first discuss the basics of pulsar timing in §2. Tests of theories of gravitation are discussed in §3, and pulsar timing arrays (PTAs) and their use as detectors of low-frequency gravitational radiation are described in §4. Pulsar timescales and the application of pulsar timing to navigation of distant spacecraft are discussed in §5. The main points of the review are briefly summarised in §6.

2. Pulsar timing

Measurement of a sequence of pulse ToAs over intervals ranging from hours to decades is the basis of precision pulsar timing. These ToAs are first transferred to an “inertial” reference frame, normally the solar-system barycentre, to remove the effects of rotation and orbital motion of the Earth. Radio-frequency dispersion resulting from the presence of ionised gas in the interstellar medium can be compensated for using observations in different frequency bands. Then, based on

¹ See the ATNF Pulsar Catalogue V1.56 (<http://www.atnf.csiro.au/research/pulsar/psrcat>) and [1]

a model for the intrinsic properties of the pulsar including its astrometric, rotational, interstellar and (if applicable) binary parameters, a predicted barycentric pulse arrival time is computed for each ToA. The difference between the observed and predicted arrival times is known as the timing “residual”. Study of the time and radio-frequency variations of these residuals is the basis of all pulsar timing. Systematic variations of the residuals indicate either errors in the pulsar model or the presence of unmodelled phenomena affecting observed ToAs. Each pulsar parameter has a distinct signature in the time and frequency domains. A least-squares fit of the these signatures to the observed residuals enables corrections to the various pulsar parameters and, possibly, the measurement of previously un-measured parameters. Examination of the remaining residuals enables investigation of new and different phenomena such as relativistic binary perturbations or gravitational waves (GWs).

One of the most basic products of long-term pulsar timing is the rate of slowdown of the pulsar rotation period $\dot{P} = -\dot{\nu}/\nu^2$, where $\nu = 1/P$ is the pulse frequency. Figure 1 shows the plot of period derivative versus pulse period for the known pulsars in the Galactic disk.² Assuming braking of the pulsar rotation by the reaction to emission of magnetic-dipole radiation, that is, electromagnetic radiation at the pulsar rotation frequency, and assuming a dipole field structure, we can compute the magnetic field at the pulsar surface

$$B_s = 3.2 \times 10^{19} \sqrt{P\dot{P}}, \quad (1)$$

where P is in seconds and B_s is in Gauss, and the “characteristic age”, that is, the time since the (back-extrapolated) pulse period was zero (see, e.g., [4])

$$\tau_c = P/(2\dot{P}). \quad (2)$$

One of the main reasons why this diagram is so useful is that different classes of pulsars generally lie in different zones on it. For example, with their short period and low spin-down rate, MSPs are located in the bottom left of the diagram. Conversely, because of their typically long periods and strong magnetic fields, magnetars are at the top right. Double-neutron-star (DNS) systems tend to lie in the gap between MSPs and normal pulsars. Young pulsars have a high probability of being detectable at high energies (optical and above) and the same applies to MSPs having a larger-than-average spindown rate. The so-called “rotating radio transients” (RRATs) (see, e.g., [5]) tend to have long periods and to lie between the magnetars and the bulk of normal pulsars. The X-ray isolated neutron stars (XINS) (see, e.g., [6]) also lie in this region.

The secular spin-down of pulsars can be described by the “braking index”, defined by

$$n = \frac{\ddot{\nu}\nu}{\dot{\nu}^2}. \quad (3)$$

Different values of n are predicted for different braking mechanisms. For example, $n = 3$ for magnetic-dipole braking, $n = 5$ for braking by emission of GWs, and braking by pulsar winds which deform the magnetosphere so that fields at the light cylinder (where the co-rotation velocity equals the velocity of light) are stronger than their dipole value have $1.0 \leq n \leq 3.0$ [4]. Because of the combined effects of random irregularities in pulsar period, especially in young pulsars, and the relatively strong $\dot{\nu}$ dependence, braking indices representing the secular braking of the pulsar have only been measured for a dozen or so pulsars [7]. Most of these are between 2.0 and 3.0 indicating some braking by a stellar wind. For example, for the Crab pulsar, the long-term average value of n is 2.342 ± 0.001 [8].

² Globular cluster pulsars are omitted as their observed \dot{P} is often affected by acceleration of the pulsar toward the cluster centre, see, e.g., [3].

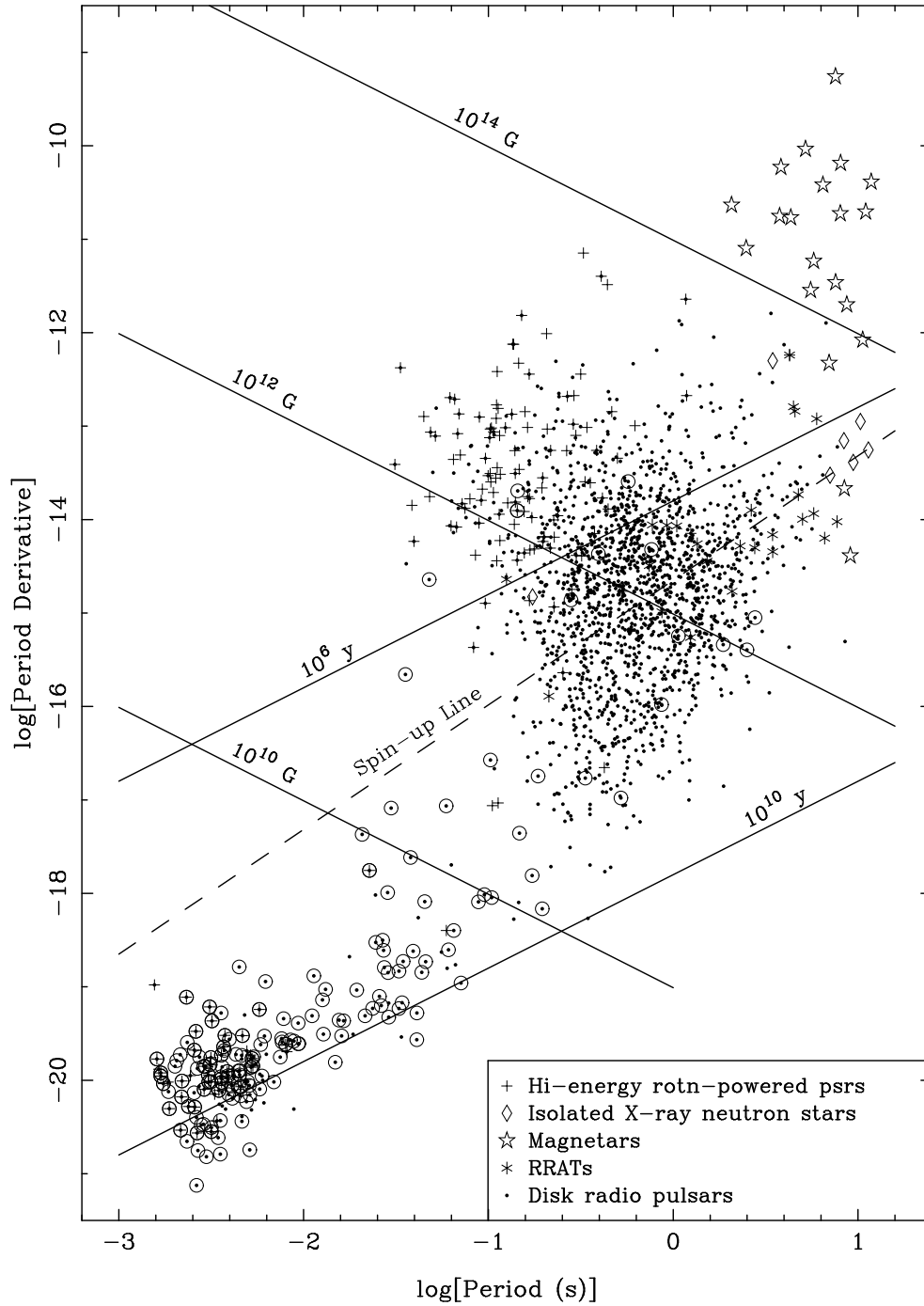


Figure 1. Plot of rate of period increase, \dot{P} versus pulse period P for known pulsars lying in the Galactic disk, that is, excluding pulsars in globular clusters and extra-galactic pulsars. Different classes of pulsars are indicated by different symbols and binary pulsars are indicated by a circle around the pulsar symbol. Lines of constant characteristic age τ_c and surface dipole magnetic field strength B_s are shown as is the maximum spin period attainable by Eddington-limited accretion of mass from a companion (see, e.g., [2]).

For young pulsars the regular slow-down is often interrupted by a sudden spin-up known as a “glitch”. About 425 of these glitches have been observed in more than 140 pulsars³ and they have relative magnitudes $\Delta\nu_g/\nu$ of between 10^{-10} and 3×10^{-5} for spin-powered pulsars. The post-glitch timing behaviour is different for different pulsars, but for large glitches generally includes an exponential relaxation toward the extrapolated pre-glitch trend followed by an enhanced linear decay of $\dot{\nu}$. This behaviour is illustrated in Figure 2.

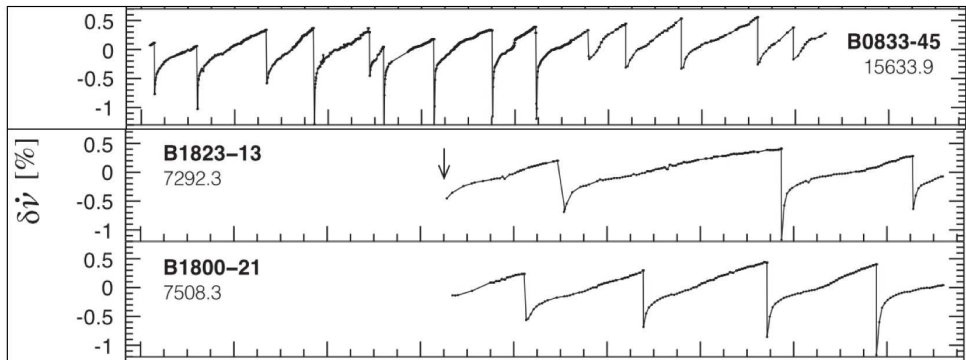


Figure 2. Time dependence of spin-down rate $\dot{\nu}$ for three young pulsars that have multiple glitches. The horizontal axis is time over the Modified Julian Date range 40000 to 57500, a total of about 48 years. The number below the pulsar name is the mean absolute spin-down rate in Hz s^{-1} . (Adapted from [7]).

During the linear decay phase, the apparent braking index is typically between 20 and 40 [7]. However, as Figure 2 shows, this does not represent the long-term evolution of $\dot{\nu}$. Following Lyne et al. [9], Espinoza et al. [7] fitted a template to the post-glitch changes in $\dot{\nu}$ to derive braking indices of 1.7 ± 0.2 , 1.9 ± 0.5 and 2.2 ± 0.6 for PSRs B0833–45, B1800–21 and B1823–13, respectively. These are all much less than the magnetic-dipole value of 3.0 and less than other well-measured secular braking indices. It should be noted, however, that Akbal et al. [10] have independently derived a braking index for the Vela pulsar (PSR B0833–45) of 2.81 ± 0.12 by fitting to the values of $\dot{\nu}$ just before a glitch rather than the post-glitch variations fitted by [7].

3. Tests of gravitational theories

The discovery of the first binary pulsar, PSR B1913+16, by Hulse and Taylor at Arecibo Observatory in 1974 [11] opened up multiple new fields of pulsar research. Important among these was tests of relativistic theories of gravitation. PSR B1913+16 was the first of the class of DNS systems (now numbering 15) that have short orbital periods, typically about a day, and relatively high eccentricities. Together with the large system mass, these properties imply large orbital velocities. For example, at periastron, the orbital velocity v of PSR B1913+16 and its companion are about 300 km s^{-1} or 0.1% of the velocity of light. Since lowest-order relativistic effects go as $(v/c)^2$, they are easily detectable as orbital modulations of the observed pulsar period. Within a few years, the first two relativistic perturbations, periastron advance and time dilation, were detected [12]. In Einstein’s general theory of relativity (GR), these depend on the masses of the two stars, together with the well-known Keplerian parameters. Consequently, the masses could be determined and both were close to $1.4 M_{\odot}$, confirming that the system consisted of two neutron stars in orbit around one another. Most importantly, measurement of the masses enabled prediction of a third relativistic term, orbital decay due to the emission of GWs from

³ ATNF Pulsar Catalogue Glitch Table

the system. This was also measured in 1979 [12] and was in accordance with the predictions of GR. Later measurements [13] show that the observed orbit decay \dot{P}_b is within 0.2% of the GR prediction. These observations are therefore, not only a confirmation of the accuracy of GR as a theory of relativistic gravitation, but also the first observational evidence for the existence of GWs. These important results were recognised by the award of the 1993 Nobel Prize in Physics to Joseph Taylor and Russell Hulse.

An even more amazing binary system, the Double Pulsar, PSR J0737–3039A/B, was discovered at Parkes in 2003 [14, 15]. This system has a orbital period of 2.4 h, about one third that of PSR B1913+16 and is a DNS system. However, unlike any other DNS system, both neutron stars are detectable as pulsars. The A pulsar, the first-born neutron star of the two, was spun up to its short period of 22 ms by accretion of mass and angular momentum from its evolving companion which subsequently collapsed to form the second neutron star. This is now detected as a relatively young pulsar (B) with a pulse period of 2.77 s.⁴ With a predicted periastron advance of $16.9^\circ \text{ yr}^{-1}$, relativistic effects are even larger than for PSR B1913+16, and hence more stringent tests can be performed [17]. Six relativistic effects have now been detected for this system, including two describing the Shapiro delay, geodetic precession of the spin axis of pulsar B [18], and a much more precise measurement of the orbital decay (Kramer et al., in preparation). These results show that GR accurately describes the system at the 0.02% level, an order of magnitude better than the PSR B1913+16 test and the most stringent test so far of GR in the strong-field regime.

Despite the success of GR in accounting for the details of ToA orbital modulations in the DNS systems, it remains possible that departures from the predictions of GR will be found in the future. There are many alternative theories of gravity and pulsars provide several mechanisms for testing the parameters of such theories. Some of these theories violate the Strong Equivalence Principle (SEP), for example, allowing differences between the gravitational and inertial masses. As pointed out by [19], this would result in bodies with different gravitational self-energy falling at different rates in an external gravitational field. For binary pulsars with white dwarf or other low-mass companions, an orbital eccentricity would be induced by the gravitational field of the Galaxy. A limit on this, expressed in terms of the parameter $|\Delta| = |m_g/m - 1|$ of $\sim 4.6 \times 10^{-3}$, where m_g and m are the gravitational and inertial masses respectively, effectively of the neutron star, has been obtained from an analysis of the orbital eccentricities of 27 pulsar – white dwarf systems with low intrinsic eccentricity [20].

Other gravitational theories predict the existence of dipolar gravitational radiation. A strong limit on this has been placed by Freire et al. [21] from an analysis of the various contributions to \dot{P}_b in the pulsar – white dwarf system PSR J1738+0333.

The recent discovery of the very interesting triple system, PSR J0337+1715, by Ransom et al. [22] has opened up the possibility of an even more stringent test of the SEP. This system consists of a 2.73-ms pulsar in a 1.7-day orbit around a $0.19 M_\odot$ white dwarf. In a co-planar orbit of period 327 days around both these stars is a somewhat more massive $0.41 M_\odot$ white dwarf. Aside from interesting questions about the orbital dynamics and origin and evolution of this system, it is possible that the gravitational field of the outer white dwarf will induce an eccentricity in the orbit of the inner white dwarf. Since the gravitational field of the outer white dwarf at the position of the inner white dwarf is about 10^6 times as strong as the Galactic gravitational field, this test is potentially much more sensitive than the SEP test based on the pulsar – white-dwarf binary systems [20].

⁴ The B pulsar became undetectable in 2008, most likely because of spin-axis precession, but it should reappear sometime within the next decade or so [16].

4. Pulsar timing arrays

Although MSPs have extremely stable periods, one cannot rule out the possibility of intrinsic variations in the observed timing parameters of a given pulsar. Uncorrected variations in interstellar propagation delays are also possible. Therefore, in order to search for extrinsic modulations due to (for example) low-frequency GWs propagating through the Galaxy, it is necessary to observe many MSPs and to search for correlated timing variations among the sample. Such a set of MSPs, widely distributed on the sky and with frequent high-precision timing observations over a long data span is known as a “pulsar timing array” (PTA). PTAs are sensitive to low-frequency (nanoHertz) gravitational waves that could be generated by orbiting super-massive black holes in the cores of distant galaxies. Although individual binary systems could be detectable, the most likely GW source to be detected by PTAs is a stochastic background generated by many such binary systems in galaxies at redshifts of between one and two [23]. Predicted amplitudes of such a background suggest that observations of about 20 MSPs over 10 years are necessary for a detection.

There are three main PTA projects around the world: the European Pulsar Timing Array (EPTA) which uses data from several large radio telescopes in Europe, the North American NANOGrav array, which uses data from Arecibo and the Green Bank Telescope, and the Parkes Pulsar Timing Array (PPTA) which uses data from the Parkes 64-m telescope in Australia. Each of these has high-precision timing data on at least 20 MSPs with data spans ranging between a few years and nearly 30 years. Typically the pulsars in each PTA are observed at intervals of 2 – 3 weeks in two or three different radio-frequency bands.

Detection of GWs by PTAs relies on the correlations between the timing signals for pulsars in different directions on the sky induced by GWs passing over the Earth. Hellings & Downs [24] showed that, for a stochastic background, the correlations depend only on the angular separation of the pulsar pairs, not their sky location. Pulsars close together on the sky have positively correlated signals but, because of the quadrupolar nature of gravitational radiation, pulsars that are in perpendicular directions have negatively correlated signals. The correlation returns to a positive value for pulsars that are diametrically opposed on the sky. GWs passing over the pulsars produce signals that are uncorrelated between the pulsars in the array, just adding a noise component to the GW signal.

Other correlated signals may exist in the data. For example, irregularities in the reference timescale (typically International Atomic Time, TAI), will have the same effect on timing residuals for all pulsars in the array. In terms of the sky distribution, this is a monopolar effect. Errors in the solar-system ephemeris used to refer the ToAs to the solar-system barycentre are equivalent to errors in the computed position of the Earth and so will have a dipolar signature on the sky. These different dependencies on sky position can be used to separate the different effects.

Up to now, there has been no positive detection of nanoHertz GWs by pulsar timing arrays. However, just by using the best few pulsars in an array, it is possible to set a limit on the strength of the GW background in the Galaxy. The best limit so far is from the PPTA as illustrated in Figure 3. This P15 limit, based on Parkes observations in the 10cm band (~ 3 GHz) of the four best-performing MSPs in the PPTA sample, effectively rules out all “standard” models for generation of a low-frequency GW background. This means that one or more of the assumptions that went into the construction of these models, for example, the merger rate of galaxies or the mass function for super-massive black holes in the cores of galaxies, is in error. Shannon et al. [25] consider that the most likely cause for the lower-than-expected GW background level is that, at a late stage in their evolution, super-massive black-hole binary systems lose energy to surrounding gas rather than to GWs. It should be remarked that recently uncovered differences in solar-system ephemerides may affect the derived GW background limits.

An analysis of the GW sensitivity of a PTA as a function of the PTA parameters [29] shows

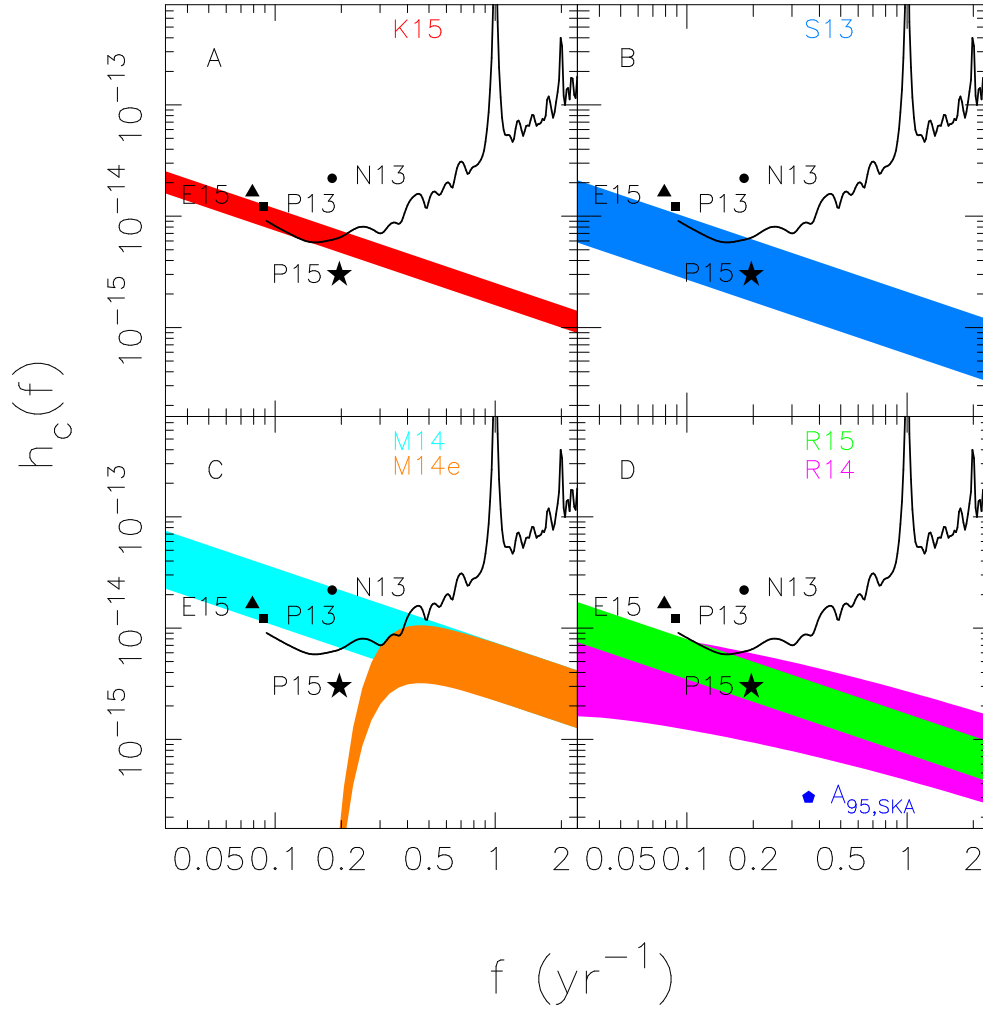


Figure 3. Limits on the characteristic strain of a GW background in the Galaxy from PTA observations. Marked points are 95% confidence limits from NANOGrav (N13, [26]), the EPTA (E15, [27]), the 2013 PPTA limit (P13, [28]), and the most recent PPTA limit (P15, [25]). Different predictions for the spectrum of the GW background are shown in the different panels. The black line is the nominal spectral sensitivity of the PPTA observations used to derive the P15 limit and the point marked $A_{95,SKA}$ gives the expected sensitivity of a PTA based on the Square Kilometre Array. (From Shannon et al., *Science*, 2015, [25]. Reprinted with permission from AAAS.)

that, when the self-noise from GWs passing over the pulsars of a PTA is significant, the most efficient way to increase the sensitivity of the array is to increase the number of pulsars in it. To this end, the three regional PTAs have combined to form the International Pulsar Timing Array (IPTA). Combined IPTA data sets for 49 pulsars are now available [30] and are starting to be used to further PTA science objectives, e.g., [31]. Other ways in which the number of pulsars in PTAs can be increased is through finding previously unknown MSPs with good timing properties in pulsar searches, e.g. [32], and through the use of new large radio telescopes such as the just-commissioned Five hundred metre Aperture Spherical Telescope (FAST) in China [33] and the Square Kilometer Array (SKA), Phase 1 of which should be operational around 2023 [34].

5. Pulsar timescales and navigation

As mentioned in the previous section, PTAs are sensitive to irregularities in the timescale to which the observations are referenced, normally either TAI or the post-corrected version of TAI, BIPMxx, where xx represents the year of creation [35]. One can invert the normal process of pulsar timing and use the pulsars to “time the timescale”, in effect establishing a “pulsar timescale”. Such a pulsar timescale differs from terrestrial timescales based on atomic frequency standards in a number of important ways:

- it is independent of terrestrial timescales
- it is based on entirely different physics – the rotation of macroscopic bodies rather than quantum processes
- it will be continuous for billions of years.

Because of the nature of pulsar timing, pulsar timescales are only competitive to (or of greater stability than) atomic timescales over long intervals, months to years and decades. With their very different basis, pulsar timescales can provide a valuable independent check on the long-term stability of terrestrial atomic timescales [36].

Figure 4 shows the results of analyses of the IPTA DR1 dataset [30] for the “common-mode” or clock term relative to TT(TAI) and to TT(BIPM15)⁵ using a frequentist (TEMPO2) method and a Bayesian method (Guo et al., in preparation). The pulsar offsets define a timescale which we label TT(IPTA16). The left panels of Figure 4 show that TT(IPTA16) has significant deviations from TT(TAI) and, within the uncertainties, is consistent with TT(BIPM15). Directly referencing the pulsar ToAs to TT(BIPM15), as shown in the right panels, confirms the agreement of the two timescales. The figure also shows that consistent results are obtained with the two analysis methods. These results demonstrate that the long-term stability of a timescale based on the best available pulsar datasets is comparable to that of the best available atomic timescales. Furthermore, we have shown that the post-corrected timescale TT(BIPM15) is indeed more stable than TT(TAI).

Another interesting application of precision pulsar timing is to navigation of spacecraft that are distant from the Earth, even outside the solar system. Pulsars can form a “celestial GPS” system – instead of assuming a fixed observatory position and solving for the pulsar parameters as in normal pulsar timing, one can analyse the ToAs from a set of pulsars with known parameters and solve for the observatory position. For spacecraft navigation, it is most practical to use an X-ray telescope on the spacecraft and to observe a sample of pulsars with significant X-ray pulsed emission. Analysis of a realistic simulation [37] has shown that position location with an accuracy of better than 20 km is possible using observations of just four MSPs. Autonomous operation of the system is possible, but accuracy is improved with updates of the pulsar parameters from Earth-based observations. It is interesting to note that in 2016 the Chinese launched a satellite, XPNAV, dedicated to exploring X-ray pulsar navigation, and that NASA’s recently launched NICER mission on the International Space Station has a project (SEXTANT) devoted to this topic as well.

6. Summary

Pulsar timing has many possible applications in physics and astrophysics. Their remarkable intrinsic period stability, especially for MSPs, their distribution throughout the Galaxy and the fact that many pulsars, including more than half of all MSPs, are in binary orbits around another star, allow explorations of theories of gravitation, properties of the interstellar medium, studies of binary and stellar evolution and many other topics. Pulsar timing arrays (PTAs) can be used

⁵ Terrestrial Time (TT) is a uniform theoretical timescale based on the value of the SI second on the Earth’s geoid. TT(TAI) and TT(BIPM15) are realisations of TT based on TAI and BIPM15 respectively.

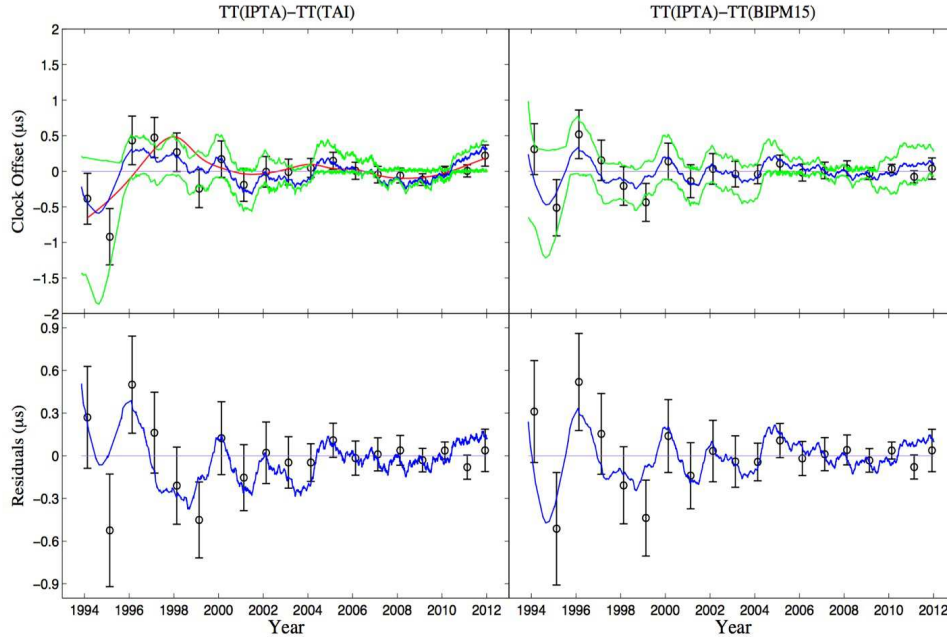


Figure 4. Offsets of the pulsar timescale TT(IPTA16) with respect to TT(TAI) (left panels) and TT(BIPM15) (right panels) derived from a frequentist analysis (black circles with error bars) and a Bayesian analysis (blue line with $1\text{-}\sigma$ error ranges in green) of the IPTA DR1 dataset. For the TT(TAI) reference, the red line gives the offset of TT(BIPM15) from TT(TAI) after subtracting quadratic terms. The lower panels show the residuals from TT(BIPM15). (Guo et al., in preparation)

as detectors of low-frequency gravitational radiation and to establish a “pulsar timescale” that is independent of terrestrial atomic timescales. In most of these areas, pulsars provide unique results and insights into the relevant physical processes. With new and more sensitive radio telescopes coming soon, the sample of pulsars that can contribute to these studies will grow, giving higher precision for existing applications and opening up new fields of research.

Acknowledgments

I thank my colleagues for their many contributions to the topics discussed and the referee for helpful suggestions.

References

- [1] Manchester R N, Hobbs G B, Teoh A and Hobbs M 2005 *AJ* **129** 1993–2006
- [2] Bhattacharya D and van den Heuvel E P J 1991 *Phys. Rep.* **203** 1–124
- [3] Freire P C C, Ridolfi A, Kramer M, Jordan C, Manchester R N, Torne P, Sarkissian J, Heinke C O, D’Amico N, Camilo F, Lorimer D R and Lyne A G 2017 *MNRAS* **471** 857–876
- [4] Manchester R N and Taylor J H 1977 *Pulsars* (San Francisco: Freeman)
- [5] Karako-Argaman C, Kaspi V M, Lynch R S, Hessels J W T, Kondratiev V I, McLaughlin M A, Ransom S M, Archibald A M, et al. 2015 *ApJ* **809** 67
- [6] Haberl F 2007 *Astrophys. Space Sci.* **308** 181–190
- [7] Espinoza C M, Lyne A G and Stappers B W 2017 *MNRAS* **466** 147–162
- [8] Lyne A G, Jordan C A, Graham-Smith F, Espinoza C M, Stappers B W and Weltevredre P 2015 *MNRAS* **446** 857–864
- [9] Lyne A G, Pritchard R S, Graham-Smith F and Camilo F 1996 *Nature* **381** 497–498
- [10] Akbal O, Alpar M A, Buchner S and Pines D 2017 *MNRAS* **469** 4183–4192

- [11] Hulse R A and Taylor J H 1975 *ApJ* **195** L51–L53
- [12] Taylor J H, Fowles L A and McCulloch P M 1979 *Nature* **277** 437
- [13] Weisberg J M, Nice D J and Taylor J H 2010 *ApJ* **722** 1030–1034
- [14] Burgay M, D’Amico N, Possenti A, Manchester R N, Lyne A G, Joshi B C, McLaughlin M A, Kramer M, Sarkissian J M, Camilo F, Kalogera V, Kim C and Lorimer D R 2003 *Nature* **426** 531–533
- [15] Lyne A G, Burgay M, Kramer M, Possenti A, Manchester R N, Camilo F, McLaughlin M A, Lorimer D R, D’Amico N, Joshi B C, Reynolds J and Freire P C C 2004 *Science* **303** 1153–1157
- [16] Perera B B P, McLaughlin M A, Kramer M, Stairs I H, Ferdman R D, Freire P C C, Possenti A, Breton R P, Manchester R N, Burgay M, Lyne A G and Camilo F 2010 *ApJ* **721** 1193–1205
- [17] Kramer M, Stairs I H, Manchester R N, McLaughlin M A, Lyne A G, Ferdman R D, Burgay M, Lorimer D R, Possenti A, D’Amico N, Sarkissian J M, Hobbs G B, Reynolds J E, Freire P C C and Camilo F 2006 *Science* **314** 97–102
- [18] Breton R P, Kaspi V M, Kramer M, McLaughlin M A, Lyutikov M, Ransom S M, Stairs I H, Ferdman R D, Camilo F and Possenti A 2008 *Science* **321** 104–
- [19] Damour T and Schäfer G 1991 *Phys. Rev. Lett.* **66** 2549
- [20] Gonzalez M E, Stairs I H, Ferdman R D, Freire P C C, Nice D J, Demorest P B, Ransom S M, Kramer M, Camilo F, Hobbs G, Manchester R N and Lyne A G 2011 *ApJ* **743** 102 1109.5638)
- [21] Freire P C C, Wex N, Esposito-Farèse G, Verbiest J P W, Bailes M, Jacoby B A, Kramer M, Stairs I H, Antoniadis J and Janssen G H 2012 *MNRAS* **423** 3328–3343
- [22] Ransom S M, Stairs I H, Archibald A M, Hessels J W T, Kaplan D L, van Kerkwijk M H, Boyles J, Deller A T, et al. 2014 *Nature* **505** 520–524
- [23] Sesana A, Vecchio A and Colacino C N 2008 *MNRAS* **390** 192–209
- [24] Hellings R W and Downs G S 1983 *ApJ* **265** L39
- [25] Shannon R M, Ravi V, Lentati L T, Lasky P D, Hobbs G, Kerr M, Manchester R N, Coles W A, et al. 2015 *Science* **349** 1522–1525
- [26] Demorest P B, Ferdman R D, Gonzalez M E, Nice D, Ransom S, Stairs I H, Arzoumanian Z, Brazier A, et al. 2013 *ApJ* **762** 94
- [27] Gerosa D and Sesana A 2015 *MNRAS* **446** 38–55
- [28] Shannon R M, Ravi V, Coles W A, Hobbs G, Keith M J, Manchester R N, Wytke J S B, Bailes M, et al. 2013 *Science* **342** 334–337
- [29] Siemens X, Ellis J, Jenet F and Romano J D 2013 *Class. Quant. Grav.* **30** 224015
- [30] Verbiest J P W, Lentati L, Hobbs G, van Haasteren R, Demorest P B, Janssen G H, Wang J B, Desvignes G, et al. 2016 *MNRAS* **458** 1267–1288
- [31] Lentati L, Shannon R M, Coles W A, Verbiest J P W, van Haasteren R, Ellis J A, Caballero R N, Manchester R N, et al. 2016 *MNRAS* **458** 2161–2187
- [32] Stovall K, Allen B, Bogdanov S, Brazier A, Camilo F, Cardoso F, Chatterjee S, Cordes J M, et al. 2016 *ApJ* **833** 192
- [33] Nan R, Li D, Jin C, Wang Q, Zhu L, Zhu W, Zhang H, Yue Y and Qian L 2011 *Intnl J. of Mod. Phys. D* **20** 989–1024
- [34] Carilli C and Rawlings S 2004 *New Astronomy Reviews*, **48** 11–12
- [35] Petrova S A 2003 *A&A* **408** 1057–1063
- [36] Hobbs G, Coles W, Manchester R N, Keith M J, Shannon R M, Chen D, Bailes M, Bhat N D R, et al. 2012 *MNRAS* **427** 2780–2787
- [37] Deng X P, Hobbs G, You X P, Li M T, Keith M J, Shannon R M, Coles W, Manchester R N, Zheng J H, et al. 2013 *Adv. Space Res.* **52** 1602–1621